Imaging the irradiance distribution in the optical near field

J. Aizenberg,[a] J. A. Rogers, K. E. Paul, and G. M. Whitesides[b]
Department of Chemistry, Harvard University, Cambridge, Massachusetts 02138

(Received 15 September 1997; accepted for publication 23 October 1997)

This letter describes the use of a sensitive photoresist for direct imaging of optical intensity profiles in near-field photolithographic experiments. A comparison between experimental patterns in exposed, developed photoresist and calculated profiles of intensity shows that this procedure provides a reliable semiquantitative image of the irradiance distribution in the near field; experiment and theory correlate adequately. A potential use of the superficial diffraction contrast recorded in photoresist as the basis for a new method of the fabrication of nanostructures is discussed. © *1997 American Institute of Physics.* [S0003-6951(97)02052-4]

Near-field ultraviolet (UV) photolithography provides a promising approach to the fabrication of sub-100 nm features.[1–4] In order to develop and optimize lithographic methods that operate in the near field, an understanding of the near-field intensity profiles is required. These profiles can be simulated, but the models are necessarily approximate and are often difficult to verify.[4–7] In this letter, we describe a convenient experimental method for recording the intensity profiles of light in lithographic experiments, using a sensitive photoresist. Photosensitive materials have been previously described as recording media for holograms.[8–10] They have also been used to characterize the optical probe in near-field microscopy.[11] We have used a negative tone photoresist (AZ 5206, Hoechst) that allows the intensity of light to be imaged directly: that is, the thickness of resist remaining following exposure and development is thickest where irradiance is highest.[12] In order to demonstrate the utility of our approach, we performed a detailed study of the irradiance distribution in the optical near field for contact-mode photolithography using elastomeric phase masks.[4,13] This recently described lithographic procedure combines the advantages of conformal-contact photolithography using amplitude masks[1,2,7] and phase-shift lithography,[14–16] and is capable of generating ~90 nm wide features with broadband ($\lambda = 330-460$ nm), incoherent light.

Figure 1 shows the theoretical profiles of intensity calculated using a simple scalar analysis[4,14,17] for a one-dimensional grating test pattern and the expected patterns in photoresist for different exposure conditions. The exposure characteristics were chosen experimentally to correspond to the $I_0 < I < I_{100}$ interval [Fig. 1(b)], where I_0 is the integrated dose of radiation below which the photoresist film is fully developable, and I_{100} is the integrated dose of radiation above which the photoresist film remains untouched by development. In this interval, the percentage of exposed film remaining is almost linearly related to the integrated radiation,[12] so that information about small differences in energy can be inferred from the thickness of the developed photoresist.

Figure 2 shows an atomic force micrograph (AFM) of the pattern in a photoresist film formed after exposure through an elastomeric phase mask[4] that had a relief structure of 2 μm lines spaced by 2 μm. The correlation between the topology of the resist surface and calculated profiles of intensity establishes that this procedure successfully images the intensity distribution in the near field.

A more thorough relative analysis of both profiles provides additional information about the deviations of the actual irradiance distribution from the simple theoretical model. Profile measurements using AFM [Fig. 2(c)] show that the photoresist film is thinner in the areas corresponding to the noncontact regions in the photomask relief than in the contact areas, while the calculated intensity patterns predict that they be identical in both regions [Fig. 2(a)]. This difference implies losses in intensity in the noncontact regions

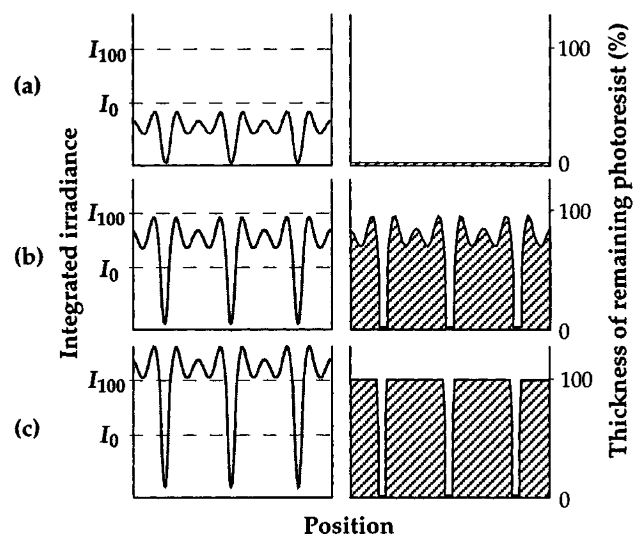

FIG. 1. Relationship between intensity profiles (left), patterns in image reversal photoresist (right), and exposure time. The intensity profile of a phase mask in conformal contact with the photoresist is taken as an input. (a) Underexposure. The whole profile of the intensity falls below the level of I_0. No pattern in the photoresist is formed. (b) Most of the intensity falls into the interval between I_0 and I_{100}. The resulting profile in the resist reproduces the actual irradiation distribution in the near field, so that the latter can be inferred from an analysis of the photoresist topography. (c) Overexposure. Most of the intensity exceeds the level of I_{100}. Under these conditions, the photoresist is insensitive to the small variations in intensity at the top of the film. In the overexposed regions, 100% of the photoresist film remains intact following the development.

[a]Electronic mail: jaizenberg@gmwgroup.harvard.edu
[b]Electronic mail: gwhitesides@gmwgroup.harvard.edu

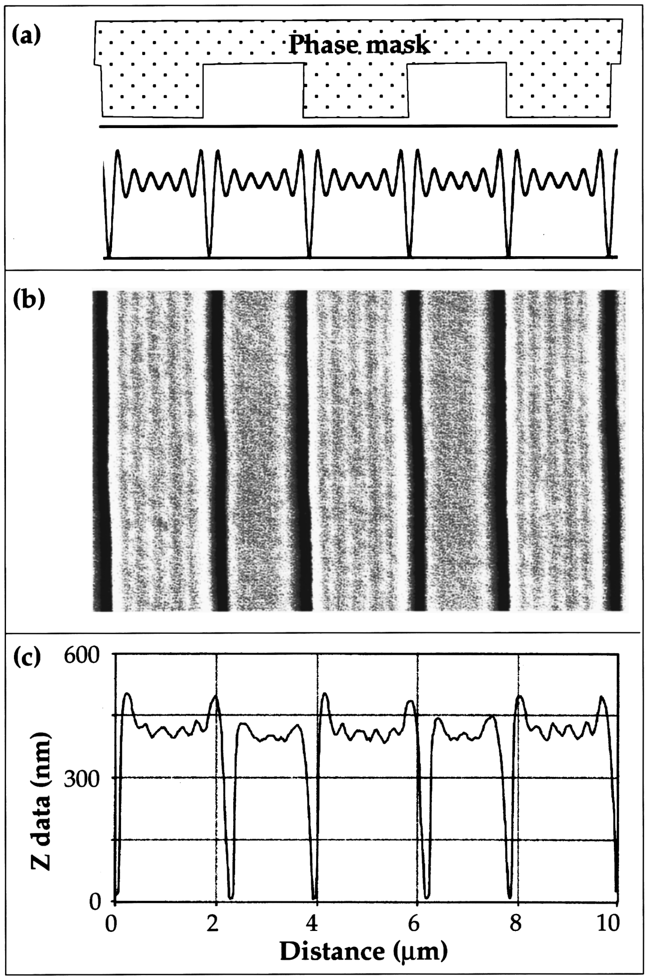

FIG. 2. Calculated profile of intensity and corresponding pattern in photoresist for the near-field photolithographic experiment, using an elastomeric contact phase mask with a grating test pattern of 2 μm lines spaced by 2 μm. The masks were prepared as described previously (see Ref. 4) by casting and curing poly(dimethylsiloxane) (PDMS, Sylgard 184, Dow Corning) against patterned rigid masters. The depth of the surface relief of the phase masks was 0.5 μm ($\sim\pi$ phase shift for wavelengths emitted by a mercury lamp). (a) Theoretical profiles of intensity calculated using a simple scalar analysis (see Ref. 4). (b) Atomic force micrograph (AFM) of the topography of the pattern in image reversal photoresist. The pattern shows a higher influence of diffraction in the regions that were in contact with the stamp than in those that were not. (c) Height profile of the sample shown in (b). Note that heights of the noncontact regions are always lower than those of the contact regions, implying that photoresist accumulates a higher integrated irradiance in the contact regions than in the noncontact regions.

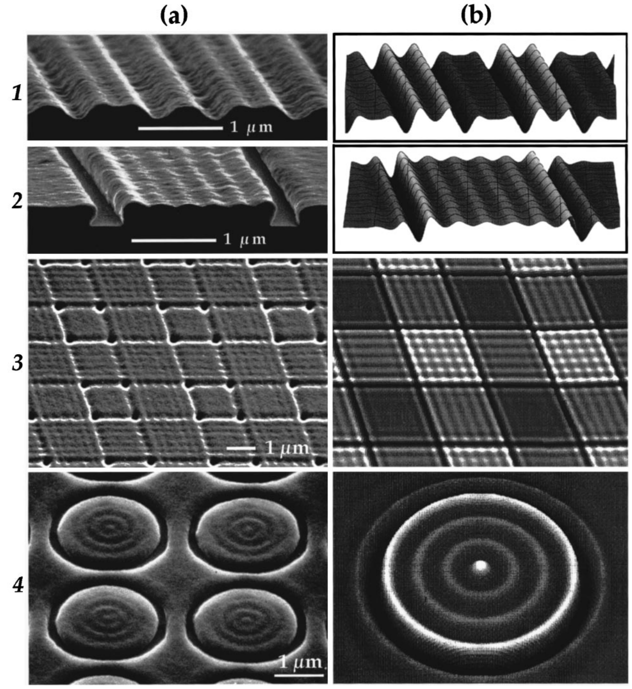

FIG. 3. Near-field irradiance distribution in contact-mode photolithography using elastomeric phase masks with different test patterns. (a) Scanning electron micrographs (SEM) of the images of the field recorded in photoresist. (b) Simulation of the profiles of intensity corrected for sagging and reflective losses at the noncontact regions. The relief structures in the elastomeric masks were composed of a grating pattern with 0.8 μm lines spaced by 0.8 μm (1); grating pattern with 2 μm lines spaced by 2 μm (2); grating pattern as in (2) exposed consecutively in two perpendicular directions (3) and raised cylinders (4).

relative to the contact regions. On the basis of these observations, we propose that reflective losses in the air gaps are one source of shadowing observed in the regions that correspond to the noncontact areas in the mask. In addition, we expected most of the distortions to derive from the sagging[18] of the noncontact regions when the elastomeric photomask comes in contact with photoresist. The effect of sagging was demonstrated using elastomeric masks of different stiffness or of different thicknesses. Stiffer or thinner masks on a rigid support that showed less sagging than thicker ones induced the formation of weak diffraction ripples in the noncontact areas.

We were able to correct the theoretical model to account for shadowing from reflective losses and sagging; these corrections improved the simulations of the irradiance distribution in the optical near field. Figure 3 shows the reconstructed calculated profiles of intensity produced in the optical near field by the elastomeric phase masks with simple and complex relief patterns, and the corresponding patterns recorded in photoresist. It is clear that the images in photoresist provide detailed information about the three-dimensional distribution of intensity of light in the optical near field and that they can be reconciled with simple theory.

The ability to record a variety of complex diffraction and interference patterns in photoresist raised the possibility of exploiting the superficial diffraction contrast as an approach to nanofabrication. Figure 4(a) shows the experimental steps used to capture the superficial image relief in low-contrast patterns; this work follows related demonstrations by Matsuda *et al.*[19] Using this method, we can extract a pattern that corresponds to the minima in intensity of light from a low-contrast photoresist profile. Figure 4(b) shows a grid pattern and an array of the 100–150 nm wide concentric rings spaced by 150–200 nm as sample structures generated from the two last profiles presented in Fig. 3. We emphasize that producing patterns of the type shown in Fig. 4 is difficult experimentally, since the quality of the struc-

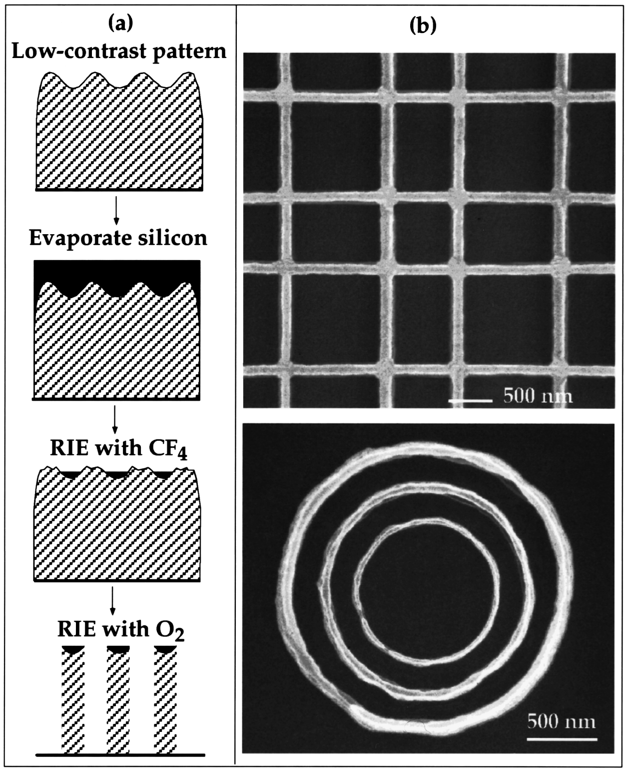

FIG. 4. (a) Schematic illustration of the process used for a superficial image emphasis (see Refs. 1 and 19) of the low-contrast diffraction patterns. A ~50 nm thick silicon film was evaporated on the photoresist surfaces bearing diffraction information. The excess silicon layer above the pattern was removed by reactive ion etching (RIE) with a plasma of CF_4. The silicon islands remaining in the regions of the diffraction minima served as a resist in RIE with O_2. (b) SEM of a grid pattern and an array of concentric rings fabricated from the last two profiles shown in Fig. 3, using the procedure outlined in (a).

tures is very sensitive to defects in the silicon layer and to the homogeneity and dose used in reactive ion etching. These structures nonetheless represent a proof of principle in a new method for the fabrication of nanostructures that cannot be produced easily by conventional lithographic techniques.

In conclusion, we believe that the procedure described here provides a sensitive method for imaging details of the optical near field. It helps to improve our understanding of the principles involved in near-field photolithography and provides means to develop and optimize photolithographic techniques.

This work was supported in part by the ONR and DARPA and by NSF (PHY-9312572). J.A.R. gratefully acknowledges the support from the Harvard University Society of Fellows. The authors thank L. Goetting and S. Shepard for their assistance in using AFM and photolithographic facilities.

[1] H. I. Smith, Superlattices Microstruct. **2**, 129 (1986).
[2] H. I. Smith, N. Efremow, and P. L. Kelley, J. Electrochem. Soc. **121**, 1503 (1974).
[3] F. Cerrina and C. Marrian, MRS Bull. **12**, 56 (1996).
[4] J. A. Rogers, K. E. Paul, R. J. Jackman, and G. M. Whitesides, Appl. Phys. Lett. **70**, 2658 (1997).
[5] B. J. Lin, in *Fine Line Lithography*, edited by R. Newman (Elsevier, North-Holland, New York, 1980), pp. 105–232.
[6] B. J. Lin, J. Opt. Soc. Am. **62**, 977 (1972).
[7] B. J. Lin, IBM J. Res. Dev. **20**, 213 (1976).
[8] G. C. Bjorklund, S. E. Harris, and J. F. Young, Appl. Phys. Lett. **25**, 451 (1974).
[9] W. T. Tsang, Appl. Opt. **16**, 1918 (1977).
[10] L. Mashev and S. Tonchev, Appl. Phys. A: Solids Surf. **26**, 143 (1981).
[11] S. Davy and M. Spajer, Appl. Phys. Lett. **69**, 3306 (1996).
[12] M. Spak, D. Mammato, S. Jain, and D. Durham, Seventh International Technical Conference on Photopolymers Ellenville, New York, 1985 (unpublished).
[13] A. Kumar and G. M. Whitesides, Appl. Phys. Lett. **63**, 2002 (1993).
[14] M. Levenson, Phys. Today **7**, 28 (1993).
[15] J. C. Langston and G. T. Dao, Solid State Technol. **3**, 57 (1995).
[16] K. O. Hill, B. Malo, F. Bilodeau, D. C. Johnson, and J. Albert, Appl. Phys. Lett. **62**, 1035 (1993).
[17] M. V. Klein, *Optics* (Wiley, New York, 1970).
[18] E. Delamarche, H. Schmid, B. Michel, and H. Biebuyck, Adv. Mater. **9**, 741 (1997).
[19] T. Matsuda, T. Ishii, and K. Harada, Appl. Phys. Lett. **47**, 123 (1985).